

Fig. S1. SEM images of the (a) Ni(OH)₂ nanosheets and (b) NiPS₃ nanosheets.

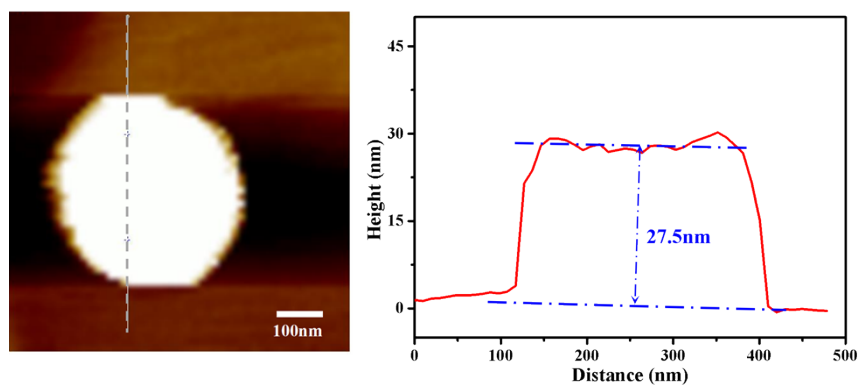


Fig. S2. AFM image of NiPS₃ nanosheets.

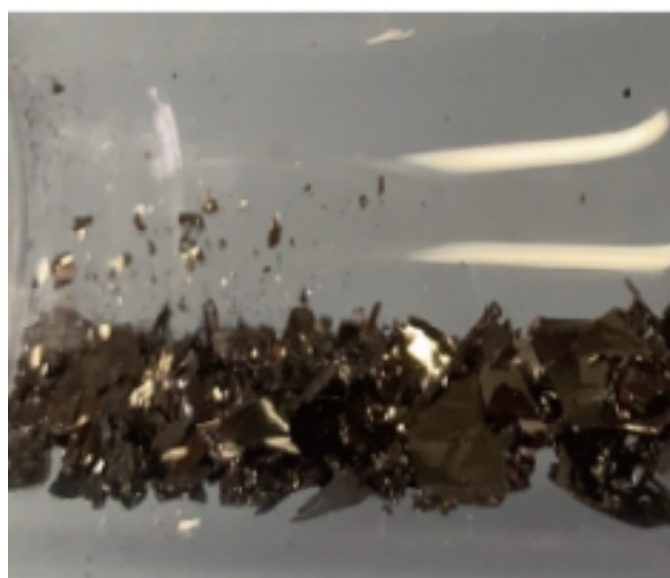


Fig. S3. Image of the bulk NiPS₃ synthesized by traditional method. Stoichiometric ratios of Ni, P and S were placed in vacuum ampoules and heated in a dual temperature zone (650°- 700°) tube furnace for five days.

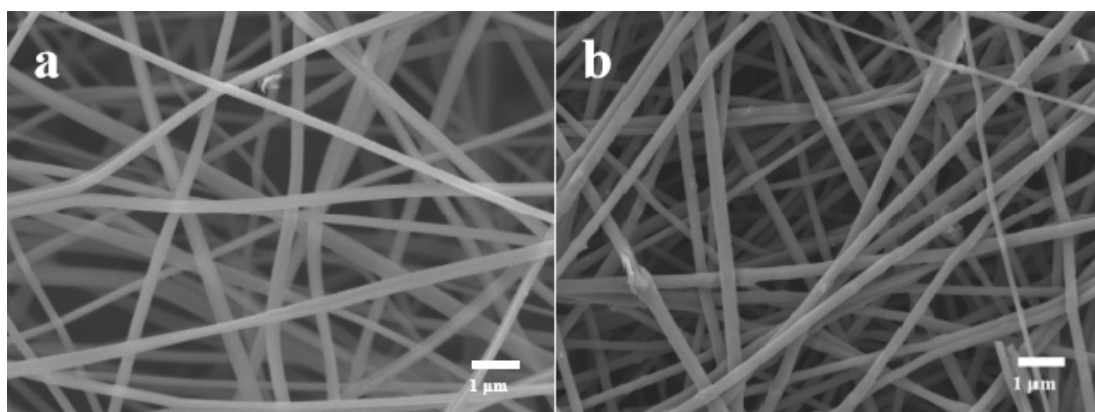


Fig. S4. SEM images of the (a) NiPS₃/CNFs and (b) NCNFs.

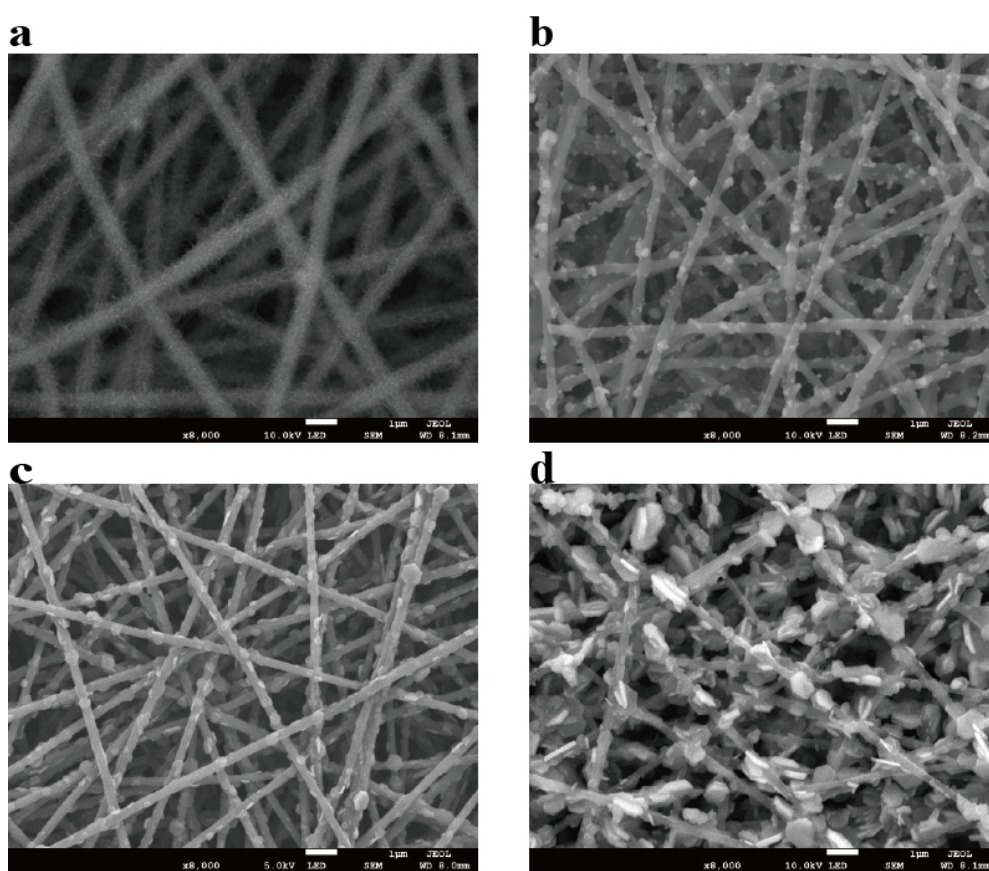


Fig. S5. SEM images of the a) Ni(OH)₂@NCNFs; b) NiPS₃@NCNFs-1 (0.5mmol NiSO₄·6H₂O), c) NiPS₃@NCNFs-2 (1mmol NiSO₄·6H₂O) and d) NiPS₃@NCNFs-3 (1.5mmol NiSO₄·6H₂O). The content of NiPS₃ nanosheets were controlled by the concentration of nickel ions.

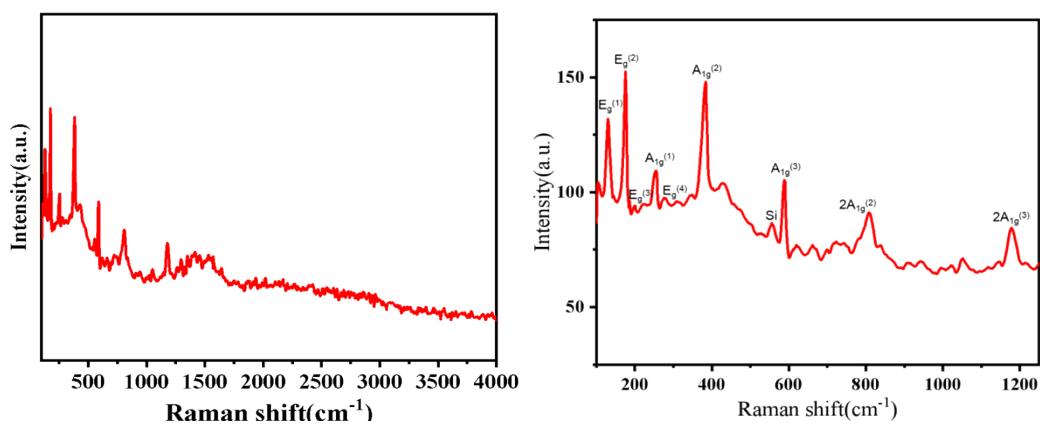


Fig. S6. Raman spectrum of NiPS₃@NCNFs, the Raman light wave number is 532nm.

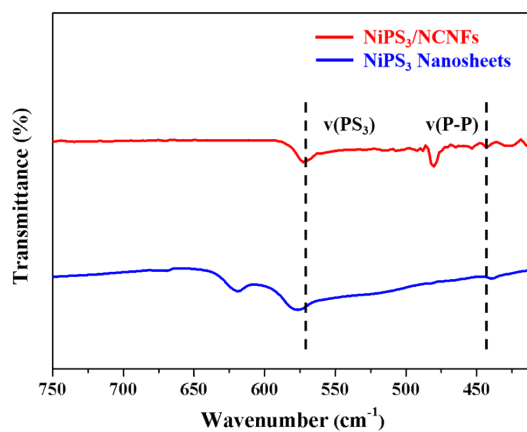


Fig. S7. FT-IR spectrum of NiPS₃@NCNFs.

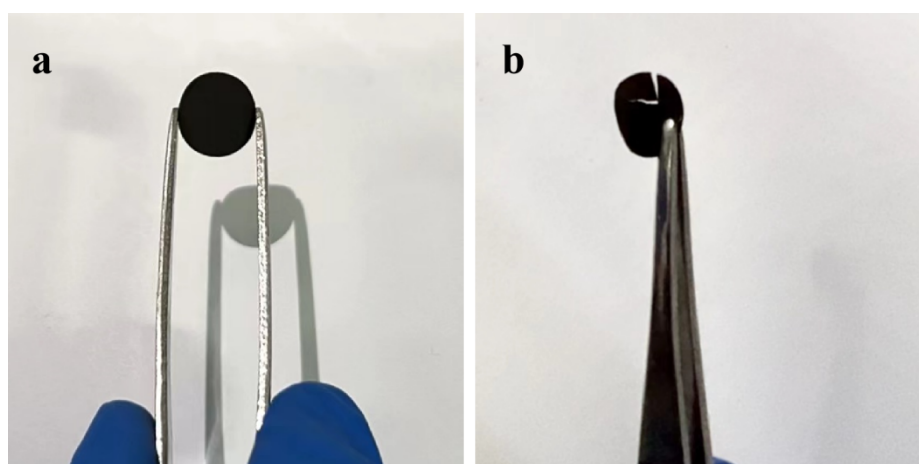


Fig. S8. (a) The NiPS₃@NCNFs after being folded in half for 300 times, (b) the cracked NiPS₃/CNFs after several folds.

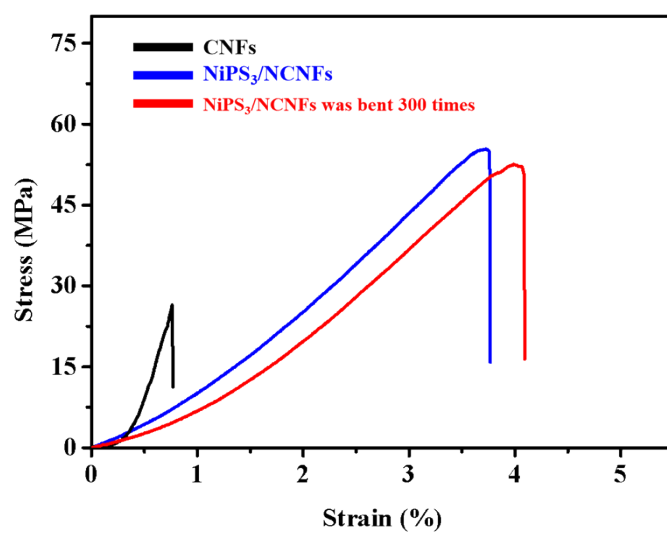


Fig. S9. The stress-strain curves of NiPS₃/CNFs, NCNFs and CNFs.

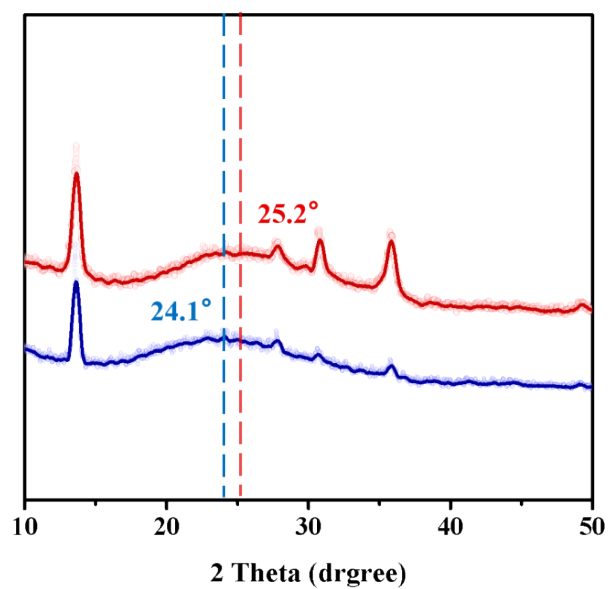


Fig. S10. XRD patterns of NiPS₃@CNFs and NiPS₃/CNFs.

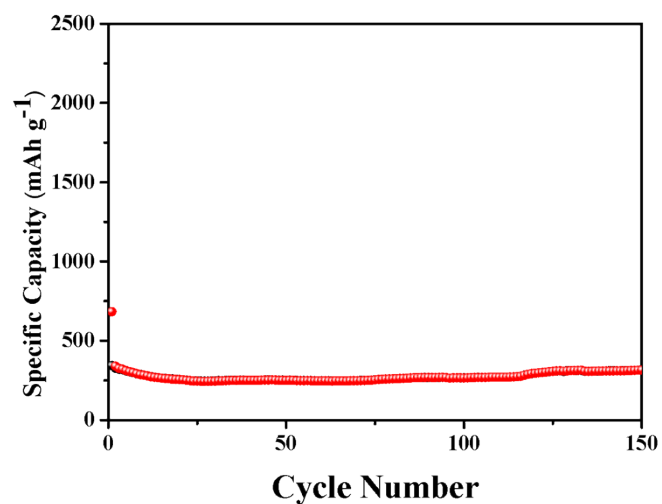


Fig. S11. Cycling performance of the NCNFs electrode at 0.1A g⁻¹.

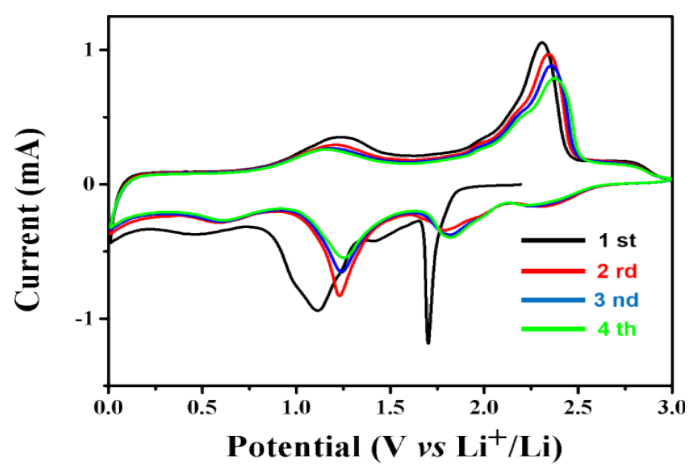


Fig. S12. CV curves of the NiPS₃@NCNFs between 0.01 -3 V at a scan rate 0.1 mV/s.

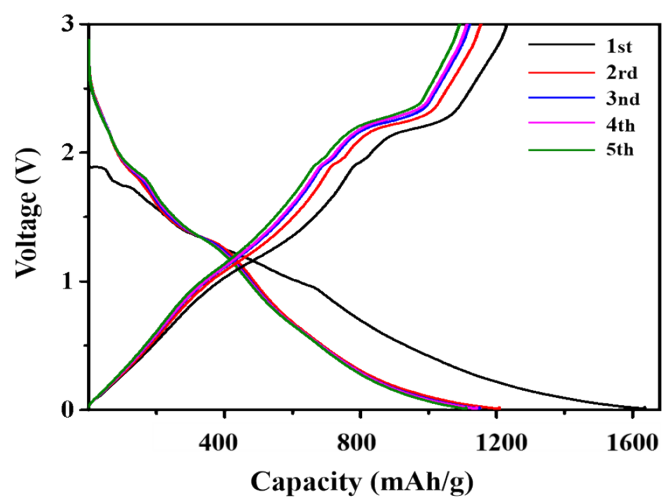


Fig. S13. Galvanostatic charge-discharge curves of the NiPS₃@NCNFs.

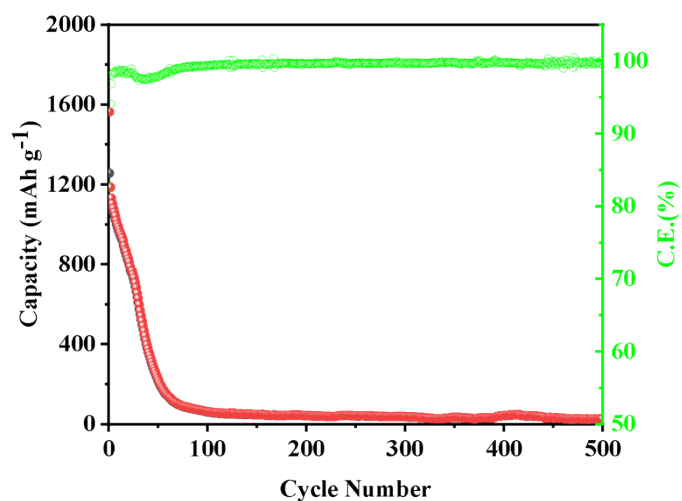


Fig. S14. Cycling performance of bulk NiPS₃ electrode at 1A g⁻¹.

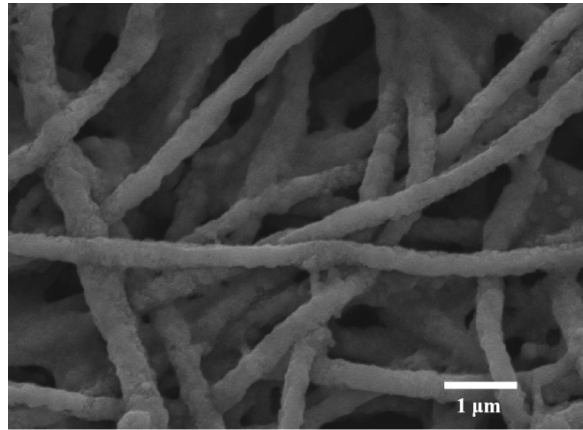


Fig. S15. SEM images of the NiPS₃/NCNFs after 1000 times charge-discharge.

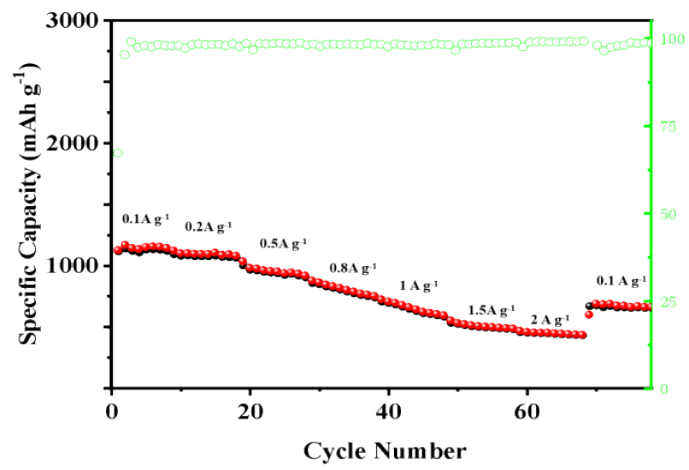


Fig. S16. Rate performances of the NiPS₃@NCNFs.

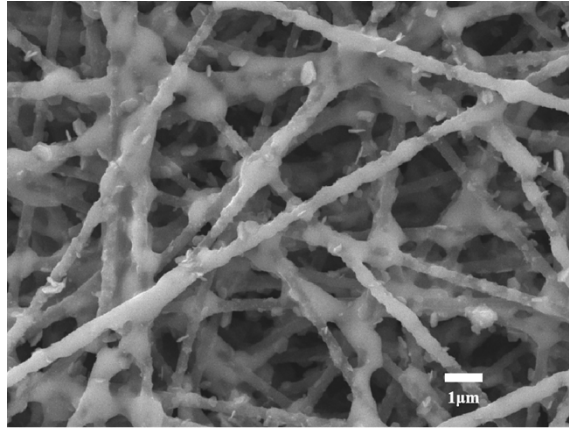


Fig. S17. SEM images of the NiPS₃@NCNFs after 3 times charge-discharge.

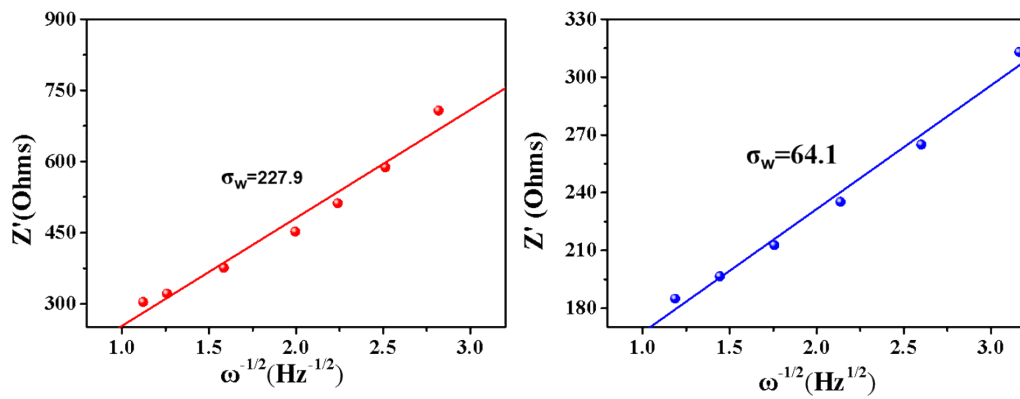


Fig. S18. The plot of real part of the impedance (Z') against the inverse square root of the angular momentum.

Table.S1. The compositions of the samples were determined by ICP. 1 mg sample was first dissolved in hot concentrated nitric acid, and the solution was diluted to 100 mL. A standard solution with Ni²⁺ concentration of 0.5, 1, 1.5, 2, and 2.5 ppm were prepared to get the standard curve.

Samples	Nickel ion concentration	Nickel ion content (per mg in electrode)	NiPS ₃ content (wt%)
NiPS ₃ @NCNFs-1	0.806mg/L	0.0806mg	25.52%
NiPS ₃ @NCNFs-2	1.088mg/L	0.1088mg	34.45%
NiPS ₃ @NCNFs-3	2.147mg/L	0.2147mg	67.99%
NiPS ₃ /CNFs	1.654mg/L	0.1654mg	52.37%
NiPS ₃ /NCNFs	1.248mg/L	0.1248mg	39.52%

Table.S2. Comparison of NiPS₃/NCNFs with other reported freestanding carbon-based electrodes.

Material	Morphology	Flexibility	Specific capacity (mAh g ⁻¹) /Current density (A g ⁻¹)	Retention capacity (mAh g ⁻¹) /Cycling number /Current density (A g ⁻¹)
NiPS ₃ /NCNFs (This work)	NiPS ₃ nanosheets embedded in CNF	Folded 300 times without creases	2156.2/0.1	893.5/1000/1
SnO ₂ /CNF ¹	SnO ₂ nanoparticle embedded in CNF	Demonstrate flexible by image	1293/0.1	754/300/1
Porous CNF ²	Carbon nanofibers	Could be bent without breaking	405/0.03	380/200/0.03
MoS ₂ /CNF ³	MoS ₂ nanosheets on CNF	Could be bent without breaking	1200/0.1	670/200/0.5
NiS/CNF ⁴	NiS nanoparticles on CNF	Demonstrate flexibility by images	1769/0.1	1021/100/0.1
SC-NF ⁵	core-shell Si/C nanofiber	Demonstrate flexibility by images	1638/0.1	720/200/0.5
SnS/C ⁶	SnS nanoparticles on CNF	Demonstrate flexibility by images	1278/0.1	330/1000/0.8
FeP@C ⁷	FeP nanotubes on CNF	Could be bent without breaking	1350/0.1	500/1100/1.5
MnOQD/CNT ⁸	MnO quantum dots on CNT	Demonstrate flexibility by images	1361/0.1	883/1000/1
SHCM/NCF ⁹	Si nanodots dispersed in carbon	Bent 180° without breaking	2583/0.1	1442/800/1
NiCoPS ₃ /NC ¹⁰	Cubic-like structure	Brittle	1312/0.1	831/1200/2

References

1. L. Xia, S. Wang, G. Liu, L. Ding, D. Li, H. Wang and S. Qiao, *Small*, 2016, **12**, 853-859.
2. L. Tao, Y. Huang, Y. Zheng, X. Yang, C. Liu, M. Di, S. Larpkiattaworn, M. R. Nimlos and Z. Zheng, *J. Taiwan Inst. Chem. E.*, 2019, **95**, 217-226.
3. J. Wang, R. Zhou, D. Jin, K. Xie and B. Wei, *Electrochim. Acta*, 2017, **231**, 396-402.
4. L. Zhang, Y. Huang, Y. Zhang, H. Gu, W. Fan and T. Liu, *Advanced Materials Interfaces*, 2016, **3**, 1500467.
5. W. Li, J. Peng, H. Li, Z. Wu, Y. Huang, B. Chang, X. Guo, G. Chen and X. Wang, *ACS Applied Energy Materials*, 2021, **4**, 8529-8537.

6. J. Xia, L. Liu, S. Jamil, J. Xie, H. Yan, Y. Yuan, Y. Zhang, S. Nie, J. Pan, X. Wang and G. Cao, *Energy Storage Materials*, 2019, **17**, 1-11.
7. X. J. Xu, J. Liu, Z. B. Liu, Z. S. Wang, R. Z. Hu, J. W. Liu, L. Z. Ouyang and M. Zhu, *Small*, 2018, **14**, e1800793.
8. S. Huang, L. Yang, M. Gao, Q. Zhang, G. Xu, X. Liu, J. Cao and X. Wei, *Electrochim. Acta*, 2019, **319**, 302-311.
9. R. Zhu, Z. Wang, X. Hu, X. Liu and H. Wang, *Adv. Funct. Mater.*, 2021, **31**, 2101487.
10. Q. Gui, Y. Feng, B. Chen, F. Gu, L. Chen, S. Meng, M. Xu, M. Xia, C. Zhang and J. Yang, *Adv. Energy Mater.*, 2021, **11**, 2003553.